THE ASTROPHYSICAL JOURNAL, 493:914–925, 1998 February 1
© 1998. The American Astronomical Society. All rights reserved. Printed in U.S.A.

NEW ROTATION PERIODS IN THE PLEIADES: INTERPRETING ACTIVITY INDICATORS

ANITA KRISHNAMURTHI,[1,2] D. M. TERNDRUP,[1] M. H. PINSONNEAULT, AND K. SELLGREN
Department of Astronomy, Ohio State University, 174 West 18th Avenue, Columbus, OH 43210; anita@astronomy.ohio-state.edu, terndrup@astronomy.ohio-state.edu, pinsono@astronomy.ohio-state.edu, sellgren@astronomy.ohio-state.edu

JOHN R. STAUFFER AND RUDOLPH SCHILD
Smithsonian Astrophysical Observatory, 60 Garden Street, Cambridge, MA 02138; stauffer@cfa.harvard.edu, rschild@cfa.harvard.edu

D. E. BACKMAN, K. B. BEISSER, D. B. DAHARI, A. DASGUPTA, J. T. HAGELGANS, AND M. A. SEEDS
Department of Physics and Astronomy, Franklin and Marshall College, P.O. Box 3003, Lancaster, PA 17604; dana@astro.fandm.edu, m_seeds@acad.fandm.edu

AND

RAJAN ANAND, BENTLEY D. LAAKSONEN, LAURENCE A. MARSCHALL, AND T. RAMSEYER
Department of Physics, Gettysburg College, Gettysburg, PA 17325; marschal@gettysburg.edu, ramseyer@goethe.uca.edu
Received 1997 April 14; accepted 1997 September 9

ABSTRACT

We present results of photometric monitoring campaigns of G, K, and M dwarfs in the Pleiades carried out in 1994–1996. We have determined rotation periods for 18 stars in this cluster. In this paper we examine the validity of using observables such as X-ray activity and the amplitude of photometric variations as indicators of angular momentum loss. We report the discovery of cool, slow rotators with high amplitudes of variation. This contradicts previous conclusions about the use of amplitudes as an alternate diagnostic of the saturation of angular momentum loss. We show that the X-ray data can be used as observational indicators of mass-dependent saturation in the angular momentum loss proposed on theoretical grounds.

Subject heading: stars: activity — stars: evolution — stars: rotation — X-rays: stars

1. INTRODUCTION

Angular momentum evolution in stars is intimately related to the stellar magnetic field, because protostars are thought to be magnetically coupled to circumstellar accretion disks, and also because stars lose angular momentum in magnetized winds. The magnetic field is related to stellar activity, including coronal activity, e.g., X-ray emission; chromospheric activity, e.g., Hα and Ca II emission; and photometric variability resulting from star spots. Unfortunately, it is generally true that stellar winds from low-mass stars, angular momentum loss, and even magnetic field strength and structure are not directly observed. Observational studies of angular momentum evolution have therefore centered on correlations between stellar activity as indicators of magnetic activity and other stellar properties, such as mass, age, and rotation rate.

The observed distributions of rotation velocities in open clusters of different ages reveal that the rate at which stars lose angular momentum on the main sequence depends both on their age and on their mass (e.g., Stauffer 1991). The angular momentum loss rate $\dot{J}$ is proportional to ωB^2 for low to moderate values of ω, where ω is the angular velocity, and B is the mean surface magnetic field (Weber & Davis 1967). As B is proportional to ω for a linear dynamo, $\dot{J}$ is proportional to ω^3 for slow rotators. If this is also true for high values of ω, then rapid rotation would be suppressed prior to the main sequence, as fast spinners would undergo heavy angular momentum loss (Pinsonneault, Kawaler, & Demarque 1990). The observation of rapid rotators on the main sequence in young open clusters, such as α Per and the Pleiades (50 and 70 Myr, respectively; Stauffer et al. 1984; Stauffer et al. 1985; Stauffer 1994) thus requires a saturation of $\dot{J}$ at high rotation rates in theories of angular momentum evolution. There is also some theoretical support for a decreased sensitivity of $\dot{J}$ to ω at higher rotation rates (Mestel & Spruit 1987; MacGregor & Brenner 1991).

It has long been known that chromospheric activity and X-ray activity are correlated with rotation among lower main-sequence stars, gradually increasing from slow rotators to rapid rotators and then reaching a plateau (Noyes et al. 1984; Rosner, Golub, & Vaiana 1985). This plateau is sometimes interpreted as resulting from a saturation in the mean surface magnetic field. The amplitude of brightness variations in low-mass stars has also been proposed as an alternate indicator of the saturation of the surface magnetic field (O'Dell et al. 1995).

There is considerable scatter in plots of stellar chromospheric and coronal activity versus rotation that is greatly reduced if activity is plotted versus the Rossby number, defined as the ratio of the rotation period $P_{\rm rot}$ to the convective overturn time $\tau_{\rm conv}$ (Noyes et al. 1984; Simon, Boesgaard, & Herbig 1985; Patten & Simon 1996). As $\tau_{\rm conv}$ depends on mass, this suggests that stellar activity in stars depends both on rotation and on mass (e.g., Patten & Simon 1996).

Reproducing the mass-dependent rapid rotation and spin-down has been a challenge for theoretical models until recently (see Krishnamurthi et al. 1997 for a review of theoretical efforts). Some models, using a constant value of the saturation threshold that depends only on the angular velocity, cannot reproduce the mass dependence of the

[1] Visiting Astronomer, Kitt Peak National Observatory, National Optical Astronomy Observatories, which is operated by the Association of Universities for Research in Astronomy (AURA), Inc., under cooperative agreement with the National Science Foundation.

[2] Current address: JILA, University of Colorado, Campus Box 440, Boulder, CO 80303.

TABLE 1

TELESCOPES AND DETECTORS

Telescope	Scale (arcsec pixel^{-1})	FOV (arcmin)	Gain (e^- DN^{-1})	Readout Noise (DN)	Linearity (DN)
NURO 0.8 m......	0.49	4.0	12.9	10.5	20,000
KPNO 0.9 m......	0.68	23.0	3.2	4.0	180,000
Lowell 1.1 m	0.38	5.0	2.3	9.0	18,000
SAO 1.2 m.........	0.65	11.0	2.8	13.0	30,000
Lowell 1.8 m	0.50	6.7	1.5	12.0	30,000

rapid rotator phenomenon (e.g., Kawaler 1987, 1988; Chaboyer, Demarque, & Pinsonneault 1995a, 1995b), while others suppress rapid rotation prior to the main sequence (e.g., Pinsonneault et al. 1990).

Some recent models (Collier Cameron & Li 1994; Barnes & Sofia 1996) have considered a mass-dependent angular momentum loss law to explain the observed distribution of rotation velocities of open cluster stars. The models of Collier Cameron & Li (1994) have their starting point on the main sequence. They use an explicit mass dependence in the scaling constant in the angular momentum loss and a very high mass-dependent saturation threshold for $\dot{J}$ [$(45–75)\omega_\odot$]. However, given these parameters, Krishnamurthi et al. (1997) find that rapid rotation is suppressed prior to the main sequence for solar analogs with saturation thresholds greater than $20\omega_\odot$. Barnes & Sofia (1996) also note that different masses require different saturation thresholds, in order to account for the ultrafast rotators in the young-cluster data. However, they use an empirical fit for $\omega_{\rm crit}$ as a function of mass. Recent models of angular momentum evolution by Krishnamurthi et al. (1997) successfully reproduce the observed distribution of rotation rates in open clusters of different ages by assuming that the angular momentum loss saturation depends on the Rossby number (and hence on mass), not on angular velocity alone. As it is known that the same mass dependence reduces the scatter in the $P_{\rm rot}$–X-ray plane (Patten & Simon 1996), this establishes a connection between theory and observation that we explore further.

In this paper we report new period measurements for 18 stars in the Pleiades, increasing the number of known rotation periods in this cluster to 51. The correlation between activity and rotation in the Pleiades and in other open clusters has long been studied using $v \sin i$ measurements (e.g., Stauffer et al. 1994). As there is now a large sample of rotation periods in the Pleiades, the correlation can be studied free of ambiguities introduced by the unknown angle of inclination. We use this larger data set of rotation periods to determine which measure of stellar activity is the best observational indicator of stellar magnetic field strengths and their saturation.

2. DATA ACQUISITION AND ANALYSIS

As part of an ongoing program to determine the photometric rotation periods for stars in open clusters, we selected targets in the Pleiades spanning a range of magnitudes from $V = 10$ ($M \sim 1.0\ M_\odot$) to $V = 16$ ($M \sim 0.4\ M_\odot$), in order to define better the correlation of activity indicators and rotation over a wide mass range. We obtained differential photometry for three sets of targets over three observing seasons (1994 October–1995 January, 1995 October–1996 January, and 1996 October), using the Kitt Peak 0.9 m telescope; the 1.8 m and 1.1 m telescopes at the Lowell Observatory in Flagstaff; the NURO 0.8 m telescope, also in Flagstaff; and the 1.2 m telescope at Mount Hopkins. Table 1 summarizes the characteristics of the various telescope and detector combinations. We opted for obtaining differential photometry, as this technique allowed us to utilize nights with marginal weather that made uniform absolute photometry difficult. This maximized the number

TABLE 2

SUMMARY OF OBSERVATIONS

Star	$N_{\rm obs}$	Dates of Observation	Telescope
HCG 20	40	1994 Oct–Dec	1, 2, 3, 4, 5
HCG 44	28	1994 Oct–Dec	2, 3, 4, 5
HCG 71	52	1995 Nov–Dec	2, 5
HCG 77	38	1994 Oct–Dec	1, 2, 3, 4, 5
HCG 103......	27	1994 Oct–Dec	2, 3, 4, 5
HCG 195......	27	1994 Oct–Dec	1, 2, 3, 4, 5
HCG 219......	31	1994 Oct–Dec	2, 3, 4, 5
HCG 380......	26	1995 Nov–Dec	2, 5
HCG 422......	26	1995 Nov–Dec	2, 5
HII 133........	61	1995 Nov–Dec	2, 4, 5
HII 174........	38	1996 Oct	1
HII 191........	43	1995 Nov–Dec	2, 4, 5
HII 212........	41	1995 Nov–Dec	2, 5
HII 253........	37	1996 Oct	1
HII 263........	54	1994 Oct–Dec	1, 2, 3, 4, 5
HII 345........	34	1996 Oct	1
HII 708........	37	1996 Oct	1
HII 738........	37	1996 Oct	1
HII 793........	37	1995 Nov–Dec	2, 4, 5
HII 883........	37	1994 Oct–Dec	1, 2, 3, 4, 5
HII 930........	63	1995 Nov–Dec	2, 4, 5
HII 1029	26	1995 Nov–Dec	2, 5
HII 1032	34	1996 Oct	1
HII 1280	32	1995 Nov–Dec	2, 5
HII 1305	32	1996 Oct	1
HII 1512	32	1994 Oct–Dec	1, 2, 3, 4, 5
HII 1532	36	1996 Oct	1
HII 1553	36	1996 Oct	1
HII 1653	36	1996 Oct	1
HII 1883	47	1994 Oct–Dec	1, 2, 3, 4, 5
	38	1996 Oct	1
HII 2147	37	1996 Oct	1
HII 2244	47	1994 Oct–Dec	1, 2, 3, 4, 5
	37	1996 Oct	1
HII 2786	34	1996 Oct	1
HII 2927	52	1994 Oct–Dec	1, 2, 3, 4, 5
HII 2966	43	1995 Nov–Dec	2, 5
HII 3197	37	1996 Oct	1

NOTES.—(1) NURO 0.8 m; (2) KPNO 0.9 m; (3) Lowell 1.1 m; (4) SAO 1.2 m; (5) Lowell 1.8 m. HII refers to the second list in Hertzsprung 1947, sometimes also referred to as HZ; HCG refers to the catalog of Haro, Chavira, & Gonzalez 1982.

TABLE 3

PROPERTIES OF THE OBSERVED STARS

Star	V[a]	$B-V$[a]	$v \sin i$[b] (km s^{-1})	log (L_x/L_{bol})[c]
HCG 20	14.23	1.37	...	...
HCG 44	16.15	...	...	...
HCG 71	14.36	1.37	...	−3.23
HCG 77	15.16	1.50	...	...
HCG 103......	16.05	...	...	−3.28
HCG 195......	15.30	1.47	...	...
HCG 219......	15.83	1.05	...	−3.11
HCG 380......	16.14	1.48	...	−3.24
HCG 422......	16.06	...	...	−2.54
HII 133........	14.14	1.31	19	−3.03
HII 174........	11.62	0.81	28	−2.94
HII 191........	14.38	1.31	...	−3.00
HII 212........	14.18	1.33	10	−3.06
HII 253........	10.66	0.65	37	−3.01
HII 263........	11.63	0.88	10	−3.33
HII 345........	11.57	0.81	18	−2.98
HII 708........	10.13	0.58	46	−3.89
HII 738........	12.30	0.81	50	−3.06
HII 793........	14.15	1.43	<9	−3.96
HII 883........	13.05	1.08	6:[e]	<−3.23[d]
HII 930........	14.08	1.22	20	−3.22
HII 1029	13.52	1.35	...	−3.88
HII 1032	11.10	0.73	36	−3.14
HII 1280	14.44	1.40	...	−2.66
HII 1305	13.52	1.15	84	...
HII 1512	13.51	1.26	9	<−3.07[d]
HII 1532	13.05	1.08	6:[e]	−3.01
HII 1553	12.49	1.08	12	...
HII 1653	13.50	1.18	21	−2.99
HII 1883	12.66	1.03	140	<−3.02[f]
HII 2147	10.83	0.78	27	−2.83
HII 2244	12.58	0.99	50	−2.82
HII 2786	10.31	0.56	25	−4.21
HII 2927	13.97	1.26	90	−3.10
HII 2966	14.74	1.46	<9	−3.37
HII 3197	12.10	1.07	33	−2.92

[a] Stauffer et al. 1991.
[b] Soderblom et al. 1993a.
[c] Stauffer et al. 1994, unless otherwise indicated.
[d] Micela et al. 1990.
[e] An uncertain value.
[f] Hempelmann et al. 1995.

of nights that could be used for observations. Each of the target fields was imaged in broadband V.

2.1. *NURO Data*

The data obtained on the NURO 0.8 m telescope were reduced separately, as the field of view was very small (4′). The first step in the reduction of the NURO data was to remove the zero-read bias and to divide by a flat-field image. Aperture magnitudes were then used to derive the differential photometry from the reduced images. The instrumental magnitudes for the target star and the brightest nearby stars were derived using the routine APPHOT in the IRAF[3] package. The star aperture was set to have a radius of 1.5 times each night's average seeing FWHM, and the sky values were measured in a contiguous annulus with a width of 1.5 FWHM. The difference in magnitude between the target and the comparison stars in the instrumental V bandpass was then computed. These differential magnitudes were then used to compute the rotation period.

Here and for the observations made on other telescopes, we made no attempt to transform the magnitudes to a standard system. It was sometimes the case with the NURO data, particularly for the brightest targets, that the nearby comparison stars were much fainter than the target star. This meant that the differential magnitude of the target could not be determined with precision. For the 1994–1995 and 1995–1996 observing seasons, we typically used the NURO data in the determination of the rotation period when the uncertainties in the differential photometry were better than 0.025 mag on average. Only the NURO group obtained data during 1996. The targets selected for observation in 1996 were expected to have short rotation periods based on high $v \sin i$ values and tentative period estimates for some of these stars from the 1994–1995 observing run.

[3] The Image Reduction and Analysis Facility (IRAF) is distributed by the National Optical Astronomy Observatories, which is operated by AURA, Inc., under contract to the National Science Foundation.

TABLE 4

NEW PERIODS REPORTED IN THIS PAPER

Star	Period (days)	Uncertainty (days)	ΔV (mag)	Uncertainty in ΔV (mag)	False-Alarm Probability
HCG 20	2.70	0.05	0.15	0.06	2.3E−4
HCG 71	2.98	0.08	0.04	0.02	7.1E−4
HII 133	1.36	0.01	0.16	0.01	2.9E−9
HII 191	3.1	0.9	0.04	0.01	5.2E−3
HII 263	4.82	0.17	0.16	0.03	1.1E−5
HII 345	0.84	0.02	0.05	0.01	5.1E−4
HII 738	0.83	0.02	0.09	0.02	5.5E−4
HII 883	7.2	0.4	0.10	0.01	1.2E−2
HII 930	1.39	0.01	0.14	0.02	2.3E−9
HII 1032......	1.31	0.03	0.12	0.01	1.1E−4
HII 1280......	0.302	0.001	0.05	0.01	1.1E−3
HII 1305......	0.389	0.002	0.10	0.02	1.7E−4
HII 1512......	8.2	0.2	0.12	0.01	5.3E−3
HII 1532......	0.78	0.02	0.06	0.01	5.1E−3
HII 1653......	0.74	0.02	0.10	0.03	3.4E−3
HII 2786......	2.21	0.13	0.07	0.02	8.5E−4
HII 2966......	4.6	0.4	0.07	0.02	2.2E−3
HII 3197......	0.44	0.01	0.04	0.01	2.3E−3

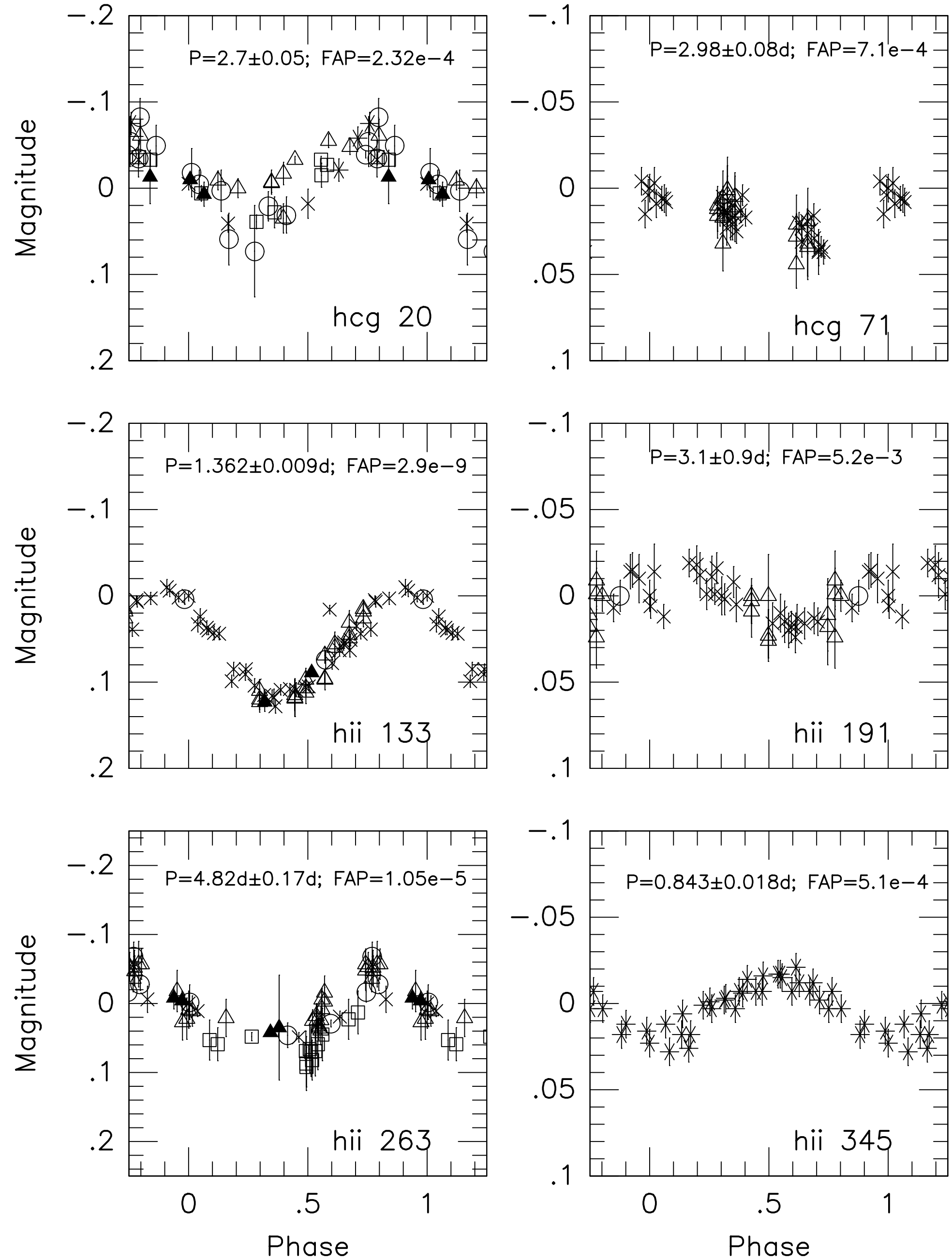

FIG. 1.—Differential light curves in *V* for Pleiades stars. The different symbols indicate data taken on different telescopes: *crosses*, data from the KPNO 0.9 m telescope; *open circles*, the SAO 1.2 m telescope; *filled triangles*, the 1.8 m Perkins telescope; *open triangles*, the 1.8 m Perkins telescope in 2 × 2 binned mode; *stars*, the NURO 0.8 m telescope; *squares*, the 1.1 m Hall telescope. Error bars indicate the photometric uncertainties.

2.2. *Other Data*

The data from the other telescopes were treated differently: we now describe this procedure. We began by doing the zero-exposure and flat-field corrections, the latter from a combination of dome and sky flats, when available. Rather than designating a set of predetermined comparison stars, we derived instrumental magnitudes for all stars on each reduced frame using version 2.0 of DOPHOT (Schechter, Mateo, & Saha 1993). We ignored all stars with central intensities that exceeded the linearity regime of the detector. This yielded the differential magnitude of each target against all the remaining stars on each frame.

To assemble the photometry for each star into a time series, we first grouped the DOPHOT output files by target star. Then, for each target star, we first generated a time series for the observations from each telescope. The final step was to tie the observations on different telescopes together by using the conventional method of scaling the magnitudes against predetermined comparison stars. We did this by identifying two to four stars located near the target Pleiades member on the CCD chip with the smallest field of view. The scatter in the relative magnitudes of the comparison stars around their mean value gave an estimate of the accuracy of this process; normally, the uncertainty

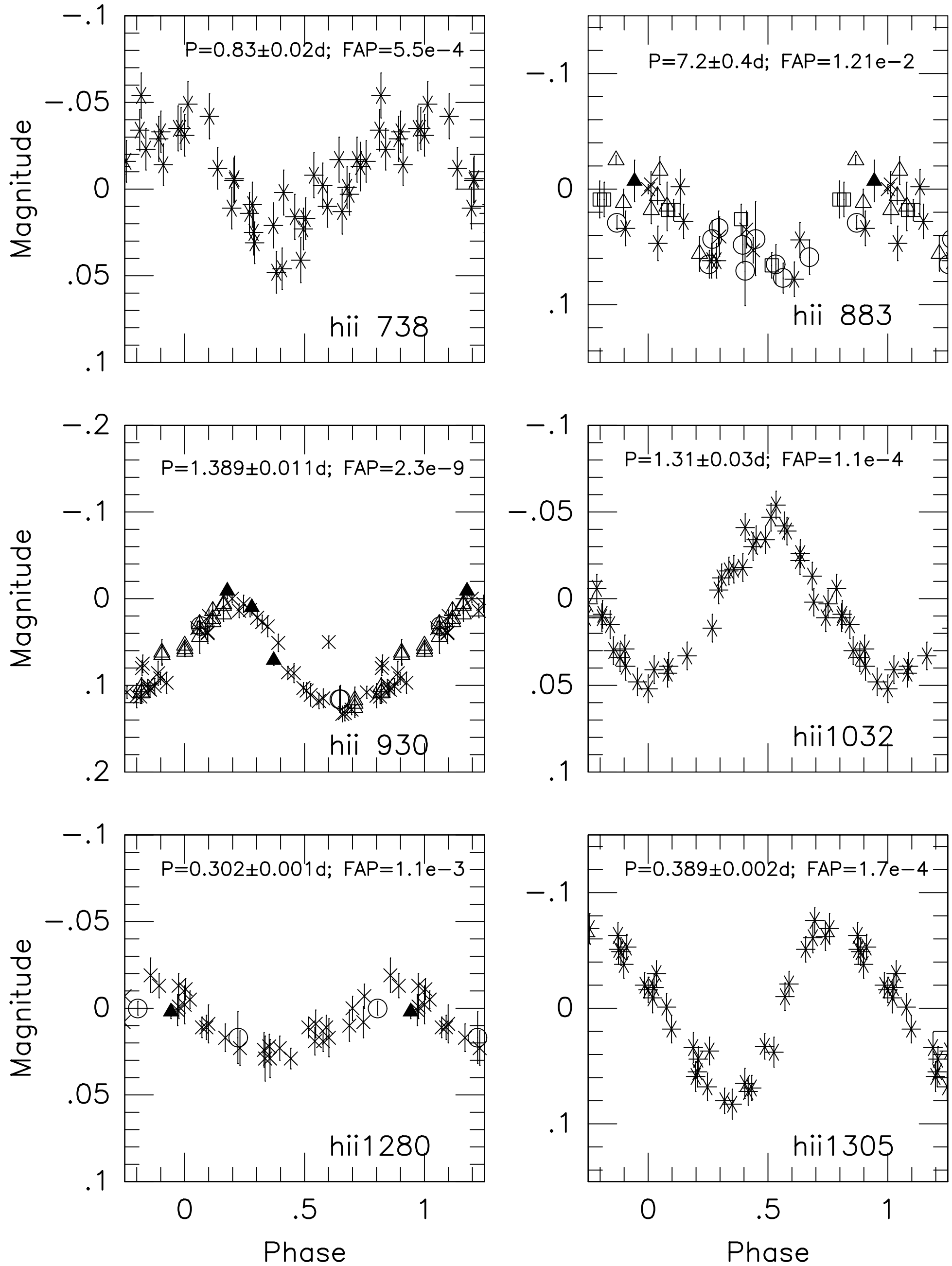

FIG. 1—*Continued*

was 0.01 mag or better. The offsets were then computed to bring the comparison stars to the scale defined by the magnitude of the target star on the zero frame for that series. This offset was applied to all the magnitudes in the time series, thus rescaling the several time series to one common magnitude scale.

2.3. *Determination of Periods*

We determined rotation periods using two different techniques. The first technique used the "Period" algorithm (Press et al. 1993) for the analysis of unevenly sampled time-series data. This routine also yields a measure of the false-alarm probability (FAP), which indicates the significance of the derived period. A small value for the FAP indicates a small probability that the peak is spurious (i.e., because of random fluctuations).

The second technique used computes the best-fitting sine wave for a given set of data. This technique utilizes the "Powell routine" (as described in Press et al. 1993) and computes the period based on the minimum χ^2 value. This routine also weights the data points by their photometric uncertainties. The uncertainty in the derived rotation period was computed to be the standard deviation of a Gaussian fit to the peak corresponding to the minimum χ^2 value. We used this routine to confirm our derived period independently. Both routines yielded the same periods for the stars reported here.

Table 2 contains a summary of the observations, where column 1 gives the name of the star observed; column 2, the number of observations per star; column 3, the date/data range of the observations; and column 4, the telescope(s) used. Table 3 lists some properties of the stars that we

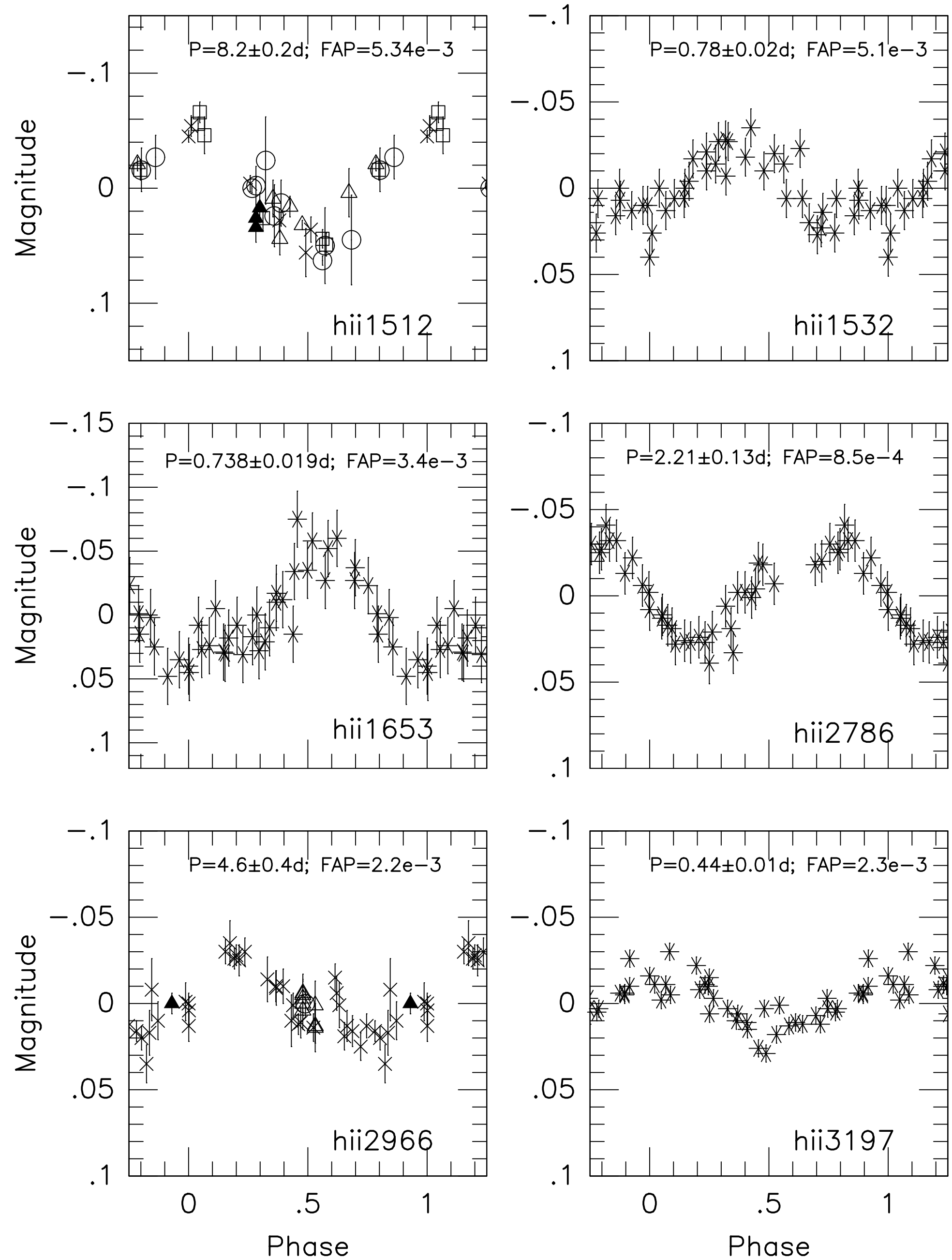

FIG. 1—*Continued*

observed: column 2 is the V magnitude; column 3, the $B-V$ color; column 4, the $v \sin i$ measurement, if known; and column 5, the logarithm of the X-ray luminosity of the stars, normalized to the bolometric luminosity. Table 4 presents the newly determined periods. The light curves are shown in Figure 1. We were successful in deriving periods for 21 of the 36 stars in our total sample. In addition to the new periods, we recovered periods for three known rapid rotators, HII 1883, HII 2244, and HII 2927. The values of 0.23, 0.56, and 0.26 days, respectively, agree with the previously determined values (van Leeuwen & Alphenaar 1982; Stauffer et al. 1987).

3. INDICATORS OF MAGNETIC FIELD SATURATION

Chromospheric and coronal emission are often used as proxies for magnetic field strength. As mentioned earlier, these activity indicators are known to be correlated with rotation and are believed to saturate at some value of rotation. Armed with a considerably larger database of rotation periods in the Pleiades, we now reexamine plots of various activity indicators versus the rotation period.

O'Dell et al. (1995) examined rotation data for G and K single dwarfs with $0.55 \leq B-V \leq 1.40$. From a study of the amplitude of variation of the stellar brightness over one rotation period ΔV, they concluded that ΔV increased with decreasing $P_{\rm rot}$ beyond the saturation threshold inferred from the chromospheric activity ($\sim$3 days for solar-type stars; Vilhu 1984). They argued that the spot coverage continues to increase with increasing rotation rate, although the chromospheric activity appears to have saturated. They proposed that the amplitude of photometric variation might be a better indicator of the saturation of the magnetic

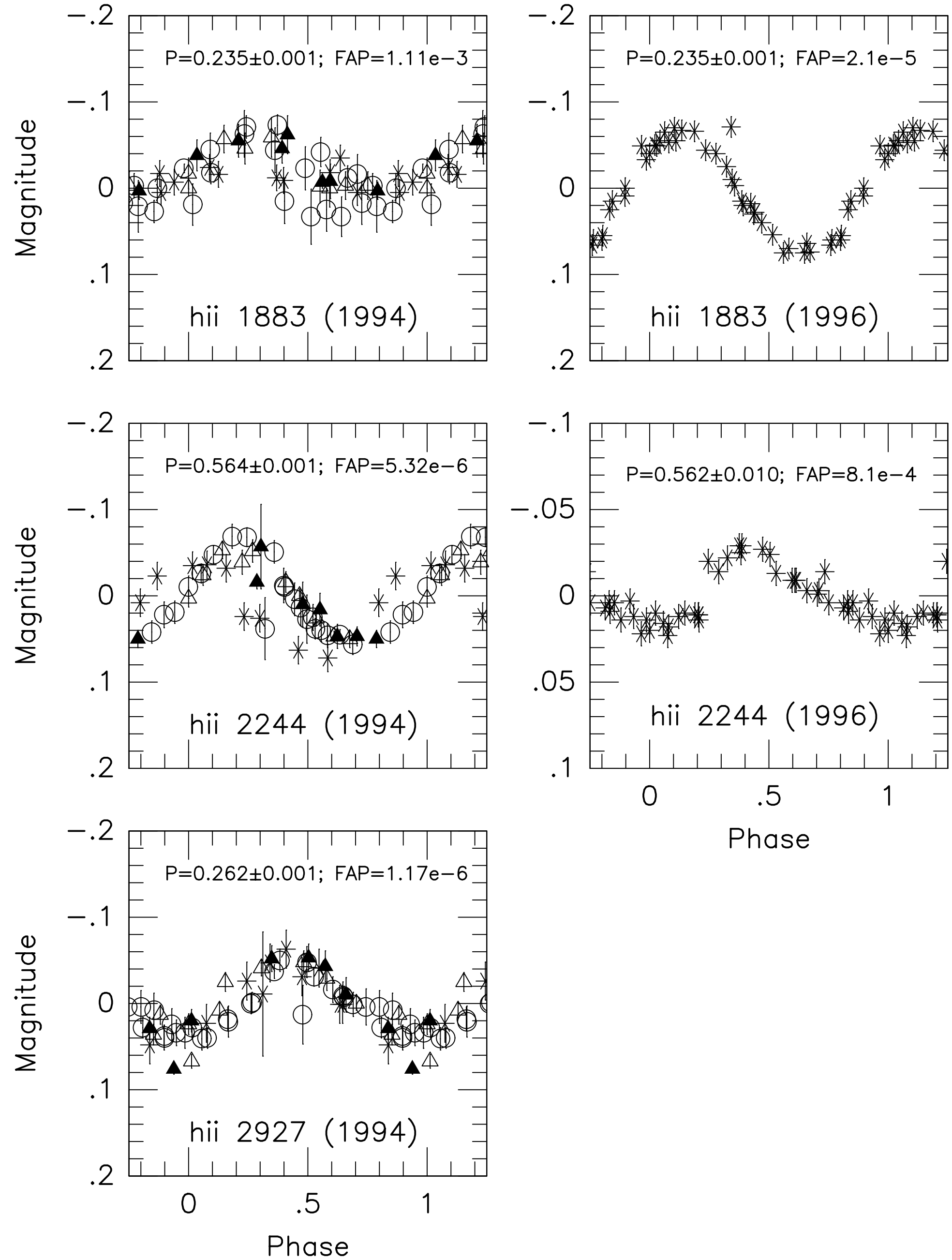

FIG. 1—*Continued*

field than the chromospheric activity and derived an upper limit on the period for saturation at $P_{rot} \sim 12$ hr. We examine this by considering the data set for the Pleiades, adding our new data to the sample, in the same color range.

As there are more X-ray data available for stars in open clusters, we begin by plotting the chromospheric (Hα and Ca II) versus coronal (X-ray) activity indicators for stars in the Pleiades in Figure 2. This demonstrates that these activity indicators are indeed correlated with each other.

In Figure 3 we plot chromospheric Hα emission, the Ca II infrared triplet (data from Soderblom et al. 1993b), coronal X-ray emission (data from Micela et al. 1990; Stauffer et al. 1994), and the amplitude of variation (compilation of older data [*open circles*] from O'Dell et al. 1995; new data [*filled circles*] from this paper) for stars in the Pleiades against the rotation period. The amplitude of variation has been defined consistently in both data sets as the difference between the maximum and minimum magnitudes. The plot shows that the activity-rotation relations are similar for both chromospheric line emission and broadband X-ray emission, with an increase in activity levels toward decreasing P_{rot}. We note here that the trends for Hα and the Ca II lines appear to have a more linear correlation with rotation than is seen in the X-ray data. However, more X-ray data are available for stars with measured P_{rot} in the Pleiades than Hα and Ca II data. The trends for all three indicators look very similar if the data set for the X-ray emission is restricted to only those stars with measurements in the other two. The additional X-ray data help to show saturation-type behavior more clearly.

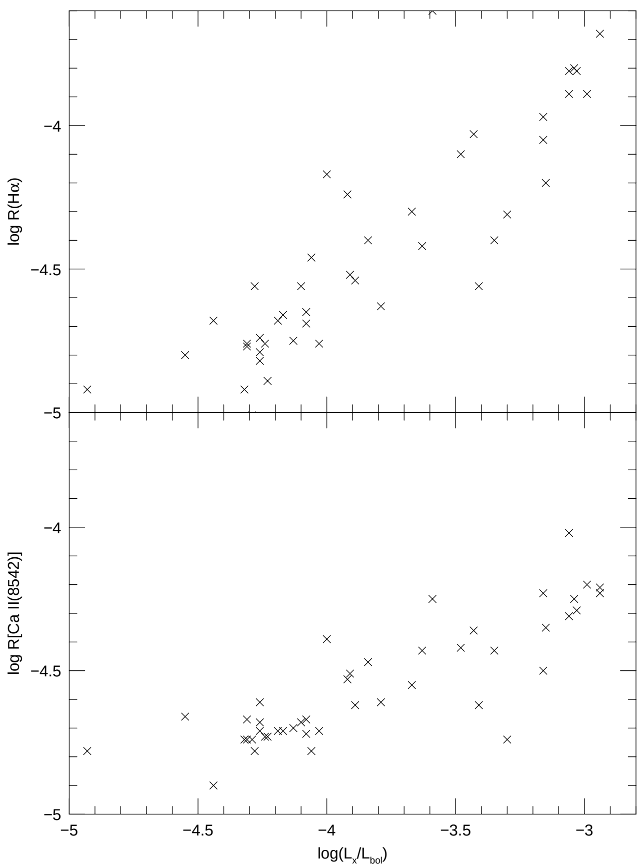

FIG. 2.—Correlation of chromospheric and coronal activity indicators for available data in the Pleiades. *Top:* Ratio of the Hα flux to the stellar bolometric flux, $R(\mathrm{H}\alpha)$, vs. the X-ray luminosity normalized to the bolometric luminosity, L_x/L_{bol}. *Bottom:* Ratio of the flux in the 8542 Å line of Ca II to the bolometric flux, R[Ca II(8542)], vs. L_x/L_{bol}. Hα and Ca II data are from Soderblom et al. (1993b); X-ray data are from Stauffer et al. (1994).

There is no trend seen for ΔV when our new rotation periods are included with the previously measured periods. It is also seen from the plot of ΔV against P_{rot} that higher amplitudes of variation exist at longer periods than seen previously (filled circles in the range $P_{\mathrm{rot}} = 2$–10 days, $\Delta V \geq 0.1$ mag.). Thus, ΔV does not increase with increasing rotation rates beyond the saturation limit of 3 days derived from chromospheric indicators (Vilhu 1984).

O'Dell et al. (1995) also noted that the coolest stars in their sample ($B-V > 1.15$) had low amplitudes ($\Delta V < 0.12$ mag), and they speculated that this effect had some physical significance. In Figure 4 we plot amplitude versus $B-V$ color, including the uncertainty in the amplitude that results from the uncertainty in the photometry. We find that four of the stars for which we have now measured P_{rot} in the Pleiades are cool stars with high amplitudes, and this result is true even when the uncertainty in the amplitudes is taken into account. Thus, there does not appear to be a decrease in ΔV for cooler stars when the sample size is increased. Furthermore, the amplitude appears to vary at different epochs for a given star. HII 1883, the fastest rotator found to date in the Pleiades, has been monitored for over 15 yr. The amplitude of this star has been found to vary from 0.04 to 0.20 mag over this time period (see Fig. 13 in Soderblom et al. 1993a). Because three or four cycles of brightness modulation are required for certainty about the derived period, most reported periods for cluster stars are for rapid rotators (P_{rot} of a fraction of a day to a couple of days), as they require shorter observing runs for accurate measurement of rotation period. Few stars with modest rotation periods (P_{rot} of 4 days and more) have had multiple amplitude measurements. By contrast, some of the rapid rotators have been studied over many years, and they are therefore more likely to have light curves from several different epochs, and they may have been observed with a high amplitude in one of those epochs. In O'Dell et al. (1995) only the largest observed amplitude was selected for analysis. Hence, we conclude that the use of ΔV as an indicator of saturation of the magnetic field is ineffective.

4. OBSERVATIONAL INDICATORS OF $\dot{J}$

We know that both the chromospheric and coronal activity indicators are better correlated, over a wide mass range, with the Rossby number N_{R} than with rotation period alone. Hence, the saturation of the chromospheric and coronal emission depends both on rotation and on mass (as the convective overturn time is a strong function of mass). Figure 5 illustrates this correlation for the Pleiades, where the chromospheric activity indicators, as well as $\log L_x/L_{\mathrm{bol}}$, are plotted against the inverse Rossby number N_{R}^{-1}, calculated using theoretical convective overturn times from Kim & Demarque (1996). We also plot ΔV versus the inverse Rossby number and note that this does not help to reduce the scatter. There does not appear to be a well-defined correlation between ΔV and P_{rot}, or between ΔV and N_{R}, for the Pleiades data set.

Figure 5 shows that ΔV varies by a factor of ~ 6 for $N_{\mathrm{R}}^{-1} = 10$–100. This is comparable with the variation in ΔV at different epochs (a factor of ~ 5) found by Soderblom et al. (1993a) for HII 1883. As X-ray activity in the Pleiades was studied by the *Einstein Observatory* and then by *ROSAT* a decade later, the scatter in X-ray activity with time for a star is observed to be a factor of at most ~ 5 (Micela et al. 1996). Figure 5 shows that the range in X-ray activity for $N_{\mathrm{R}}^{-1} = 10$–100 is a factor of ~ 40. Thus, while it is possible that ΔV depends on P_{rot} or N_{R}^{-1}, the dependence is masked by the scatter, unlike the X-ray activity.

As shown by Figure 5, the X-ray activity is very well correlated with the inverse Rossby number, plateauing at $N_{\mathrm{R}}^{-1} \sim 20$. In their theoretical models of angular momentum evolution in solar-type stars, Krishnamurthi et al. (1997) found that a mass-dependent angular momentum loss rate best reproduced the distribution of rotation rates seen in open clusters. The mass dependence used in their models was precisely this Rossby scaling. Thus, the Rossby number parameterizes the saturation threshold required both by theory (to explain the rotation distributions of open clusters) and by observation (to describe best the X-ray and chromospheric activity). Hence, the saturation of X-rays in open cluster stars may be used as an observational indicator of the saturation of the angular momentum loss law. Identifying the precise level of X-ray saturation and its mass dependence will help to pin down the level at which the angular momentum loss saturates. This is crucial and should be a goal for ground-based and space-based studies to determine rotation periods and X-ray activity levels.

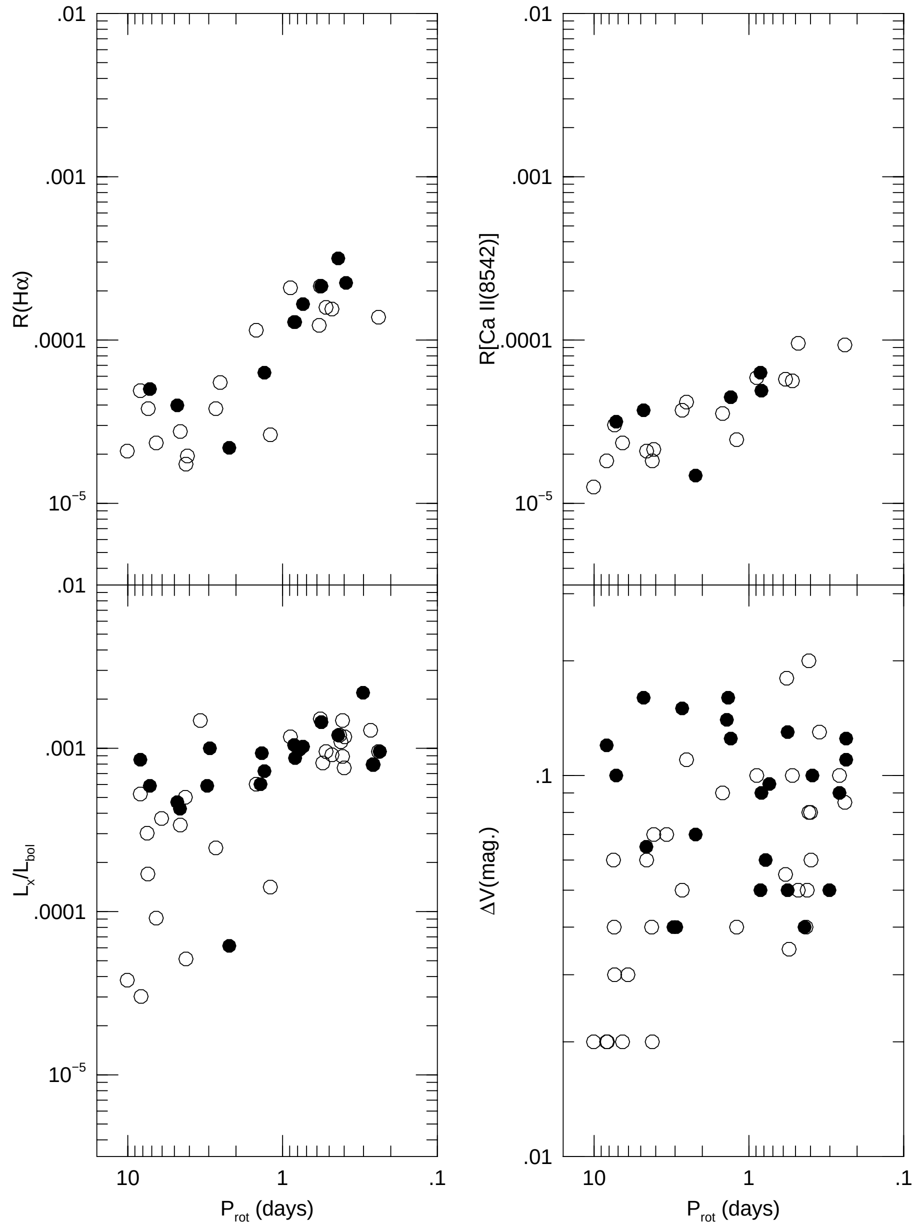

FIG. 3.—Activity indicators for Pleiades stars vs. rotation period P_{rot}. *Top*: Chromospheric Hα emission and Ca II infrared triplet at 8542 Å. *Bottom*: X-ray luminosity normalized to the bolometric luminosity, L_x/L_{bol}, and the amplitude of variation at V resulting from starspot modulation ΔV. Hα, Ca II, and X-rays increase with decreasing rotation period. Hα and Ca II data are from Soderblom et al. (1993b); X-ray data are from Stauffer et al. (1994). Rotation period data: *open circles*, previously existing periods from Magnitskii (1987), Stauffer et al. (1987), Prosser et al. (1993, 1995, as compiled by O'Dell et al. (1995); *filled circles*, our new periods.

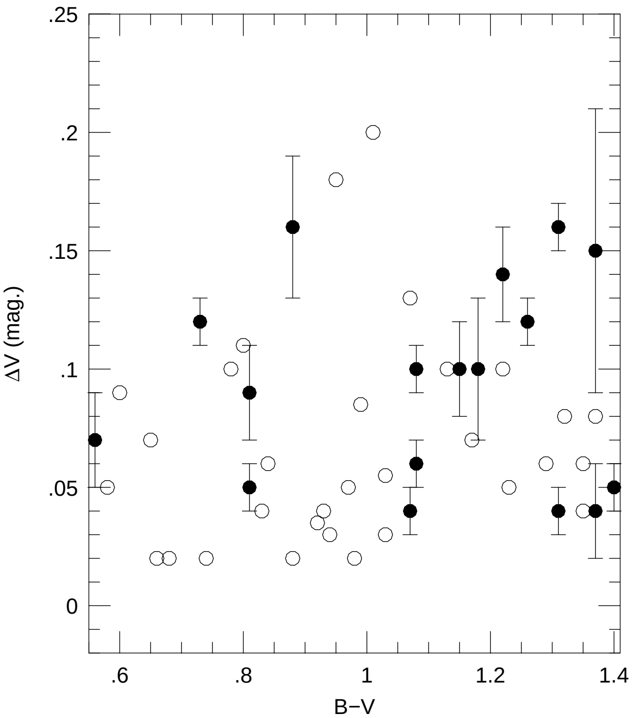

FIG. 4.—Amplitude of photometric variation ΔV vs. $B-V$ color for Pleiades stars. *Open circles:* Periods compiled by O'Dell et al. (1995); *filled circles:* our new periods. Error bars represent the uncertainty in the amplitude determination resulting from the photometric uncertainties.

5. CONCLUSIONS

We have presented results of our photometric monitoring campaign of G, K, and M dwarfs in the Pleiades. X-ray emission has long been known to correlate roughly with rotation period, and it has been shown to correlate well with Rossby number (defined as the ratio of the rotation period to the convective overturn time, hence a function both of rotation and of mass). We conclude that the mass-dependent saturation of the X-ray emission is consistent with the mass-dependent saturation of the angular momentum loss required theoretically. Thus, we now have an observable that may be used to determine the threshold for angular momentum loss saturation. Additional periods and X-ray data obtained in the turnover region would aid in determining the functional form of the mass dependence. The lack of slowly rotating, cool, high-amplitude variable stars in previous observations had led to some discussion on the use of the photometric amplitudes as an alternate diagnostic of saturation. However, our discovery of such stars in the Pleiades shows that the distribution of the amplitudes does not indicate a different saturation threshold from that inferred from X-rays.

The mass of the stars included in our sample ranges from roughly 0.5 to 1.2 $M_{\odot}$. There is strong observational evidence that the mass dependence of the angular momentum loss law continues for lower mass stars (Stauffer et al. 1997; Jones, Fischer, & Stauffer 1996). Establishing the mass dependence of the saturation in activity for the lower main sequence may provide valuable clues for models of stellar winds. In particular, there seems to be no obvious change in the rotation properties of stars at the boundary between stars with radiative cores and those that are fully convective ($\sim 0.25\ M_{\odot}$).

A Rossby-scaled angular momentum loss law would imply high saturation thresholds for stars more massive than 1.0 $M_{\odot}$, where the convective overturn timescale decreases rapidly with increasing mass. A loss law of the form used by Krishnamurthi et al. (1997) would suppress rapid rotation in higher mass stars. There is little evidence for angular momentum loss in either the pre–main sequence or the main sequence for stars with $M > 1.6\ M_{\odot}$, while there is pre–main-sequence spin-down in the intermediate-mass regime ($M \sim 1.3$–$1.6\ M_{\odot}$; Wolff & Simon 1997). The highest mass models (1.2 $M_{\odot}$) considered by Krishnamurthi et al. (1997) spun down too quickly when compared to the cluster data, when a Rossby scaling for the saturation threshold was adopted. This may indicate either a change in the nature of the wind for stars more massive than 1 $M_{\odot}$ or a defect in the particular angular momentum loss prescription of Krishnamurthi et al. for high saturation thresholds.

We close by noting that there are alternate means of limiting the angular momentum loss rates for rapid rotators. Buzasi (1997) has proposed a systematic tendency toward polar activity for lower mass stars as a possible explanation of the mass dependence of angular momentum loss (see also Solanki, Motamen, & Keppens 1997). There are also other effects, such as a tendency toward a more complex magnetic field geometry at high field strengths, which could act to cap the angular momentum loss rates for rapid rotators (e.g., Mestel 1984). A good observational database of activity and rotation measurements as a function of mass and time may prove valuable for evaluating the relative merits of the different classes of theoretical models.

Observations were made with the Perkins 1.8 m reflector of the Ohio Wesleyan and Ohio State Universities at Lowell Observatory, the 1.1 m Hall telescope at Lowell Observatory, the 1.2 m Mount Hopkins telescope at Whipple Observatory, and the Lowell Observatory 0.8 m telescope, which, under an agreement with Northern Arizona University and the NURO Consortium, is operated 60% of the time as the National Undergraduate Research Observatory. We thank the Kitt Peak National Observatory staff for their technical support during our runs on the 0.9 m telescope, as well as R. Mark Wagner and Ray Bertram at Lowell Observatory for their technical support and expertise. We thank Jodie Dalton, Greg Piecuch, and Phil Turcotte for assistance in observations at the NURO telescope and in the reduction of the NURO data. We also wish to thank Charles Prosser at CfA for obtaining some measurements for this project and Sidney Wolff for providing valuable comments. A. K. wishes to thank S. M. Long for discussions and help with the period-finding routines. Franklin and Marshall College and Gettysburg College thank the University of Delaware/Bartol Research Institute's NASA Space Grant College Consortium for support of NURO membership and partial support of student travel. Financial support for this project was provided by NSF grant AST 95-28227 to D. T. and M. H. P., an Ohio State University Seed Grant to M. H. P., and by NASA LTSA program grant NAGW-2698 to J. R. S.

We would also like to thank the anonymous referee for constructive comments that improved the paper significantly.

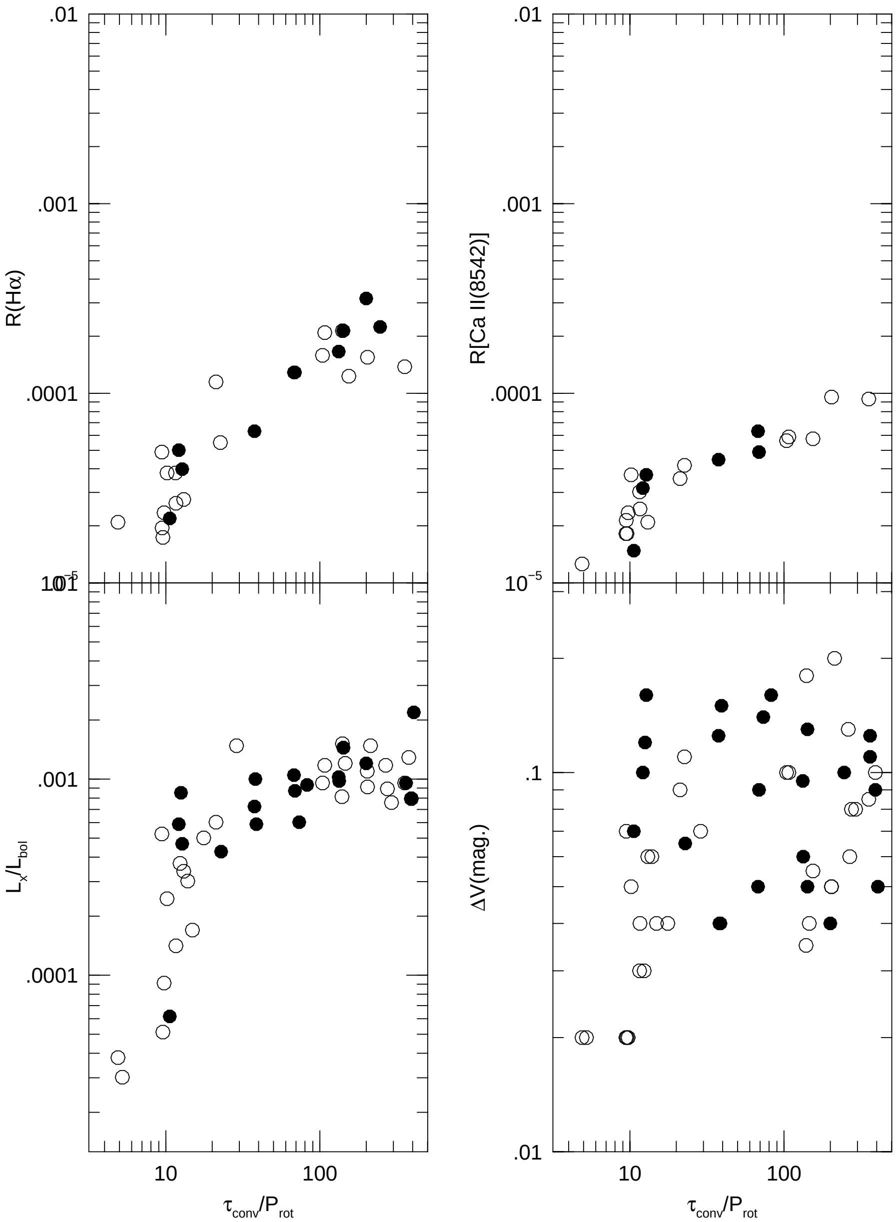

FIG. 5.—Activity indicators for Pleiades stars vs. the log of the inverse Rossby number, P_{rot}/τ_{conv}, where τ_{conv} is the convective overturn timescale. *Top:* Chromospheric Hα emission and Ca II infrared triplet at 8542 Å. *Bottom:* L_x/L_{bol} and ΔV. Symbols same as in Fig. 3.

REFERENCES

Barnes, S., & Sofia, S. 1996, ApJ, 462, 746
Buzasi, D. L. 1997, ApJ, 484, 855
Collier Cameron, A., & Li, J. 1994, MNRAS, 269, 1099
Chaboyer, B., Demarque, P., & Pinsonneault, M. H. 1995a, ApJ, 441, 865
———. 1995b, ApJ, 441, 876
Haro, G., Chavira, E., & Gonzalez, G. 1982, Boll. Obs. Tonantzintla y Tacubaya, 3, 3
Hempelmann, A., Schmitt, J. H. M. M., Schultz, M., Ruediger, G., & Stepien, K. 1995, A&A, 294, 515
Hertzsprung, E. 1947, Ann. Leiden Obs., 19, No. 1A
Jones, B. F., Fischer, D. A., & Stauffer, J. R. 1996, AJ, 112, 1562
Kawaler, S. D. 1987, PASP, 99, 1322
———. 1988, ApJ, 333, 236
Kim, Y. C., & Demarque, P. 1996, ApJ, 457, 340
Krishnamurthi, A., Pinsonneault, M. H., Barnes, S., & Sofia, S. 1997, ApJ, 480, 303
Macgregor, K. B., & Brenner, M. 1991, ApJ, 370, L39
Magnitskii, A. K. 1987, Soviet Astron. Lett., 13, 451
Mestel, L. 1984, in Cool Stars, Stellar Systems and the Sun, 3d Cambridge Workshop, ed. S. L. Baliunas & L. Hartmann (Heidelberg: Springer), 49
Mestel, L., & Spruit, H. C. 1987, MNRAS, 226, 57
Micela, G., Sciortino, S., Kashyap, V., Harnden, F. R. Jr., & Rosner, R. 1996, ApJS, 102, 75
Micela, G., Sciortino, S., Vaiana, G. S., Harnden, F. R. Jr., Rosner, R., & Schmitt, J. H. M. M. 1990, ApJ, 348, 557
Noyes, R. W., Hartmann, L. W., Baliunas, S. L., Duncan, D. K., & Vaughan, A. H. 1984, ApJ, 279, 763
O'Dell, M. A., Panagi, P., Hendry, M. A., & Collier Cameron, A. 1995, A&A, 294, 715
Patten, B., & Simon, T. 1996, ApJS, 106, 489
Pinsonneault, M. H., Kawaler, S., & Demarque, P. 1990, ApJS, 74, 501
Press, W. H., Teukolsky, S. A., Vetterling, W. T., & Flannery, B. P. 1993, Numerical Recipes (Cambridge: Cambridge Univ. Press), 569
Prosser, C. P., et al. 1993, PASP, 105, 1407
———. 1995, PASP, 107, 211
Rosner, R., Golub, L., & Vaiana, G. S. 1985, ARA&A, 23, 413
Schechter, P. L., Mateo, M., & Saha, A. 1993, PASP, 105, 1342
Simon, T., Boesgaard, A. M., & Herbig, G. 1985, ApJ, 293, 551
Soderblom, D. R., Stauffer, J. R., Hudon, J. D., & Jones, B. F. 1993a, ApJS, 85, 315
Soderblom, D. R., Jones, B. F., Balachandran, S., Stauffer, J. R., Duncan, D. K., Fedele, S. B., & Huden, J. D. 1993b, AJ, 106, 1059

Solanki, S. K., Motamen, S., & Keppens, R. 1997, A&A, 325, 1039
Stauffer, J. R. 1991, in NATO ASI Ser. 340, Angular Momentum Evolution in Young Stars, ed. S. Catalano & J. R. Stauffer (Dordrecht: Kluwer)
———. 1994, in ASP Conf. Ser. 64, Proc. 8th Cambridge Workshop, Cool Stars, Stellar Systems and the Sun, ed. J.-P. Caillault (San Francisco: ASP), 163
Stauffer, J. R., Balachandran, S. C., Krishnamurthi, A., Pinsonneault, M., Terndrup, D. M., & Stern, R. A. 1997, ApJ, 475, 604
Stauffer, J. R., Caillault, J.-P., Gagne, M., Prosser, C. P., & Hartmann, L. W. 1994, ApJS, 91, 625
Stauffer, J. R., Hartmann, L. W., Burnham, J. N., & Jones, B. F. 1985, ApJ, 289, 247
Stauffer, J. R., Hartmann, L., Soderblom, D. R., & Burnham, N. 1984, ApJ, 280, 202
Stauffer, J., Klemola, A., Prosser, C., & Probst, R. 1991, AJ, 101, 980
Stauffer J. R., Schild, R. A., Baliunas, S. L., & Africano, J. L. 1987, PASP, 99, 471
van Leeuwen, F., & Alphenaar, P. 1982, Messenger, 23, 15
Vilhu, O. 1984, A&A, 133, 117
Weber, E. J., & Davis, L. Jr. 1967, ApJ, 148, 217
Wolff, S. C., & Simon, T. 1997, PASP, 109, 759